Plant Physiology Preview. Published on May 30, 2012, as DOI:10.1104/pp.112.196345

Running head:

Rice Phosphate Transporter OsPht1;1

Corresponding author:

Guohua Xu,

[1]State Key Laboratory of Crop Genetics and Germplasm Enhancement, [2]Key Laboratory of Plant Nutrition and Fertilization in Low-Middle Reaches of the Yangtze River, Ministry of Agriculture, Nanjing Agricultural University, Nanjing 210095, China.

Tel/Fax: 0086-25-84396246; Email: ghxu@njau.edu.cn

Journal research area:

Environmental Stress and Adaptation

A constitutive expressed phosphate transporter, OsPht1;1, modulates phosphate uptake and translocation in Pi-replete rice

Shubin Sun, Mian Gu, Yue Cao, Xinpeng Huang, Xiao Zhang, Penghui Ai, Jianning Zhao, Xiaorong Fan, Guohua Xu*

[1]State Key Laboratory of Crop Genetics and Germplasm Enhancement, [2]Key Laboratory of Plant Nutrition and Fertilization in Low-Middle Reaches of the Yangtze River, Ministry of Agriculture, Nanjing Agricultural University, Nanjing 210095, China

*For correspondence (Email: ghxu@njau.edu.cn; Tel/Fax: 0086-25-84396246)

Financial sources:

This work was supported by the China 973 Program (2011CB100300), China National Natural Science Foundation, the National Program on R&D of Transgenic Plants, PAPD project in Jiangsu Province of China, 111 project (No. B12009) and the Ph.D. Programs Foundation of Ministry of Education of China (20090097110038).

Abstract

A number of phosphate (Pi) starvation or mycorrhizal regulated Pi transporters belonging to Pht1 family have been functionally characterized in several plant species, whereas functions of the Pi transporters which are not regulated by changes in Pi-supply is lacking. In this study, we show that *OsPht1;1* (*OsPT1*), one of the 13 Pht1 Pi transporters in rice, was expressed abundantly and constitutively in various cell types of both roots and shoots. OsPT1 was able to complement the nH^+/Pi co-transporter activities in a yeast mutant defective in Pi-uptake. Transgenic plants of *OsPT1* over-expression lines and RNA-interference knockdown lines contained significantly higher and lower P concentration, respectively, compared to that of wild-type control, in Pi-sufficient shoots. These responses of the transgenic plants to Pi supply were further confirmed by the changes of depolarization of root cell membrane potential, root hair occurrences, ^{33}P uptake rate and transportation, as well as P accumulation in young leaves at Pi-sufficient level. Furthermore, *OsPT1* expression was strongly enhanced by mutation of Phosphate Over-accumulator 2 (*OsPHO2*), but not by Phosphate Starvation Response 2 (*OsPHR2*), indicating that OsPT1 is involved in OsPHO2-regulated Pi pathway. The results indicate that OsPT1 is a key member of Pht1 family involved in Pi uptake and translocation in rice under Pi-replete condition.

Introduction

Phosphorus (P) is one of the key mineral elements indispensable for plant growth and development. It is a structural component of nucleic acids and phospholipids and play important roles in energy transfer, signal transduction, photosynthesis and respiration (Plaxton and Carswell 1999). Pi is taken up by plant roots from the soil and translocated within the plant *via* phosphate transporters (PiTs) (Raghothama, 1999).

A large number of the genes that encode phosphate transporters (PiTs) have been identified from different plant families, including *Arabidopsis*, cereals, legumes and *Solanaceous* species (Paszkowski, 2006; Chen et al., 2007; ; Bucher, 2007; Ai et al., 2009; Nagarajan et al., 2011; Jia et al., 2011). Majority of them showed expression either exclusively or predominately in the roots, and transcript levels were strongly induced by low-Pi supply or by inoculation with arbuscular mycorrhiza (Mudge et al., 2002; Paszkowski et al., 2002; Javot et al., 2007; Ai et al., 2009). In *Arabidopsis*, three of nine PiTs belonging to the Pht1 family have been functionally characterized by using T-DNA insertion mutants. AtPht1;1 and AtPht1;4 have been shown to be responsible for Pi acquisition under both high and low Pi conditions (Misson et al., 2004; Shin, et al., 2004). The double mutant of both AtPht1;1 and AtPht1;4 showed a 75% reduction in Pi uptake capacity as compared to WT plants (Shin, et al., 2004). Recently, Nagarajan et al. (2011) reported that *Arabidopsis pht1;5-1* mutant had higher shoot P content compared to wild-type (WT), while the P content in roots was reduced under Pi-replete condition, suggesting that Pht1;5 may mobilize Pi between source and sink tissues. In addition, Preuss et al. (2010) explored the characteristics of the low-affinity barley phosphate transporter PHT1;6 using the *Xenopus laevis* oocyte expression system, implying that it may play a Pi-transport role at Pi-sufficient condition in plant.

We previous reported that in rice two Pi-starvation enhanced Pht1 members, OsPT2 and OsPT6, have different functions and kinetic properties (Ai et al., 2009). OsPT6 plays a broad role in Pi uptake and translocation throughout the plant, whereas OsPT2 is a low affinity PiT expressed abundantly in Pi starved roots to facilitate transport of Pi from roots to shoot (Ai et al., 2009). Liu et al. (2010) reported that OsPT2 was responsible for most of the over-accumulation of Pi in shoots of *OsPHR2* over-expression lines under Pi-sufficient condition. In addition, we detected that another Pi-regulated Pht1 member *OsPht1;8* (*OsPT8*) is expressed in various tissues and organs and is involved in Pi homeostasis in rice (Jia et al., 2011).

In the present work, we investigated the functions of *OsPht1;1* (accession number AF536961, referred as *OsPT1* here) in rice. Our results showed that the expression pattern of *OsPT1* is constitutive independent of Pi supply. The P concentration in the shoots increased significantly in *OsPT1* over-expression lines and decreased in *OsPT1-RNAi* lines under Pi-sufficient condition. We also report the responses of root hair development, root cell membrane potential, Pi uptake rate and distribution in Pi-replete rice to alteration of OsPT1 expression.

Results

OsPT1 is expressed in both roots and shoots of rice independent of Pi supply condition

The expression of *OsPT1* was investigated by semi-quantitative reverse transcription (RT)-PCR in both roots and shoots at the seedlings grown under different Pi levels. *OsPT1* was found to be abundantly expressed in the roots and shoots of rice under both Pi-sufficient and -deficient conditions (Fig. S1). To further confirm this result, quantitative RT-PCR was carried out by using a housekeeping gene, *actin* (accession number AB047313), as a control. As shown in Fig. 1A, the non-alteration of *OsPT1* transcript level in the roots and shoots of the seedlings by change of Pi-supply (Fig. 1A) was consistent with the results obtained by semi-quantitative RT-PCR (Fig. S1), confirming that *OsPT1* is constitutively expressed in rice.

To analyze the tissue specific expression and Pi responsiveness of *OsPT1* in rice, we generated transgenic rice plants carrying the β-glucuronidase (GUS, Jefferson et al., 1987) as a reporter gene. The 5' fragment of 2768 bp immediately upstream of the translation start for *OsPT1* was amplified and used to drive GUS expression. The expression of GUS driven by ubiquitin promoter was used as a positive control. As shown in Fig. 1B, GUS driven by *OsPT1* promoter was abundantly expressed in various cells of roots, root-shoot junctions and leaves under both Pi-sufficient and -deficient conditions. The expression of *OsPT1* in roots and the root-shoot junctions was not only in epidermal cells which are the dominant sites for uptake of Pi from soil solution, but also throughout the cortical and stele cells (Fig. 1B, a, b, c, d, g, h, i and j), suggesting that it functions in both Pi uptake and translocation in rice. *OsPT1* was also abundantly expressed in epidermal, mesophyll and stele cells in the leaves, irrespective of Pi supply (Fig. 1B, e, f, k and l). There was weak GUS expression in the spikelets and the emerging buds (Fig. S2).

To confirm the correlation between the *OsPT1* expression pattern by PCRs and the GUS staining, we performed *in situ* hybridization with the *OsPT1* antisense probe in the roots and leaves of WT plant. The labeling of epidermis and cortex layers, central cylinder in the root sections was observed, and there was no obvious difference under different Pi-supply (Fig. 1C). Also, a similar signal in the leaves was observed under Pi-sufficient or -deficient conditions (Fig. 1C). The patterns of labeled signals were in agreement with the PCR and reporter gene expression patterns described above.

OsPT1 was able to complement nH^+/Pi co-transporter activities in a yeast mutant

To obtain biochemical evidence for the function of OsPT1, we performed the complementation analysis using the yeast mutant MB192 which is defective in gene *PHO84* that encode a high-affinity Pi transporter on the plasma membrane. The transformed cells with either *OsPT1* or empty vector were grown in yeast nitrogen base (YNB) medium containing different concentrations of Pi and bromocresol purple as a pH indicator. A color shift from purple to yellow indicated the acidification of the liquid medium over a period of 24h. In comparison with the cells of both WT and mutant MB192, the transformants expressing *OsPT1* (Yp112-*OsPT1*) could restore their growth at 20 μM Pi (Fig. 2A). At 60 μM Pi concentration, there was no obvious difference in growth between the transformant and WT cells (Fig. 2A).

The pH dependence of Pi transport by OsPT1 was measuring over a range of pH values. Growth of MB192 yeast strain expressing *OsPT1* was optimal near neutral pH medium. It has a sharp pH optimum at 6.5, whereas the WT have a broad pH optimum (Fig. 2B).

To determine the kinetic properties of OsPT1, Pi-uptake experiments using ^{33}Pi were performed in the transformed yeast mutant. Uptake rates of ^{33}Pi at different Pi concentrations showed that Pi uptake mediated by OsPT1 followed Michaelis-Menten kinetics, exhibiting an apparent mean *Km* of 177 μM Pi (Fig. 2C). The data suggest that OsPT1 has lower Pi-affinity than its homolog OsPT8 (*Km*=23 μM Pi) which is also abundantly expressed in various rice tissues (Jia et al., 2011).

Change in the expression of *OsPT1* altered P concentration in Pi-replete shoots

To characterize the function of OsPT1 in Pi uptake and translocation in rice, we generated *OsPT1* over-expression lines using ubiqitin promoter (*OsPT1*-Ox) and knockdown lines by RNA interference (*OsPT1*-Ri) in the background of a *japonica* cultivar Nipponbare *via Agrobacterium*-mediated transformation. Based on semi-quantitative RT-PCR and real time quantitative RT-PCR analyses, we selected the two lines of *OsPT1*-Ox (*Ox1* and *Ox2*) and *OsPT1*-Ri (*Ri1* and *Ri2*), respectively, for further characterization. The transcript level of *OsPT1* was increased by about 2.3-fold in *OsPT1*-Ox lines and decreased by about 51% in *OsPT1*-Ri lines in comparison to its expression in WT (Fig. 3A). *OsPT1* expression was not significantly regulated by Pi-supply level in the transgenic rice plants (Fig. 3A). Meanwhile, we detected the relative expression of the genes that encode Pi-transporters belonging to Pht1 family in shoot of *OsPT1*-Ox and wild-type plants using real time quantitative RT-PCR. *OsPT8* and *OsPT4* were significantly and moderately up-regulated, respectively. Others PTs detected were down-regulated (Fig. S3).

In comparison with WT, *OsPT1*-Ox and *OsPT1*-Ri contained 76.3% higher and 27.9% lower P concentration in the shoots grown under Pi -sufficient supply on the average, respectively (Fig. 3B), whereas no significant differences of P concentration in their shoots under Pi-deficient supply (Fig. 3B). No significant differences of P concentration in roots were detected between the *OsPT1*-Ox, *OsPT1*-Ri and WT under both Pi-sufficient and -deficient conditions with only exception of higher Pi in the Pi-deficient *OsPT1*-Ox1 lines (Ox1) (Fig. 3C).

We used Ox1 and Ri1 to further examine the effects of *OsPT1* over-expression or knockdown on Pi uptake rate and translocation at the different levels of Pi supply. As expected, Pi concentrations both in the shoots and roots of transgenic and WT plants were increased as the increases of Pi concentration in the culture solution (Fig. 4A and B). It is remarkable that the degree of shoot Pi concentration increase by *OsPT1*-Ox in comparison with WT was enlarged as the increases of external Pi supply concentration (Fig. 4A). However, there was no significant difference of Pi concentration in the roots of *OsPT1*-Ox1, *OsPT1*-Ri1 and WT irrespective of Pi supply levels (Fig. 4B).

Change in the expression of *OsPT1* altered Pi uptake rate and distribution in Pi-replete rice

To precisely determine the contribution of OsPT1 to Pi acquisition and translocation, the uptake and distribution assay of ^{33}P radioisotope was performed using *OsPT1*-Ox, *OsPT1*-Ri and WT plants pretreated with sufficient Pi. As shown in Fig. 5A and Fig. S4, *OsPT1*-Ox transgenic plants (Ox1, Ox2) showed the strongest ^{33}P signals relative to WT, whereas in the *OsPT1*-Ri transgenic plants, ^{33}P signals decreased from the base to the top of the plants (Ri1, Ri2) relative to WT. ^{33}P uptake rates of the roots of *OsPT1*-Ox1 and *OsPT1*-Ox2 transgenic plants were 18.3 and 21.6 nmol min $^{-1}$g^{-1} DW, which is 34% and 67% higher than that of WT, respectively (Fig. 5A). In contrast, ^{33}P

uptake rates of the roots of *OsPT1*-Ri1 and *OsPT1*-Ri2 transgenic plants was 8.15 and 9.32 nmol $min^{-1}g^{-1}$ DW, about 31-40% lower than that of WT (Fig. 5A). The relative amount of ^{33}P translocation from roots to the shoots was moderately increased after 24h Pi uptake in *OsPT1*-Ox plants, whereas it decreased in *OsPT1*-Ri plants (Fig. 5B). There were no significant differences of the uptake rates and distribution ratio of ^{33}P between roots and shoots at Pi-deficient condition (10 μM) for *OsPT1*-Ox, *OsPT1*-Ri and WT (data not shown).

Root acquired Pi must eventually be loaded into the apoplastic space of the xylem and transported to the shoot. In order to confirm that OsPT1 contributed to Pi transportation from roots to shoots, we measured the Pi concentration in the xylem sap of stems. The result showed that the Pi concentration in the xylem sap of *OsPT1*-Ox plants dramatically increased than that of WT, by nearly 2-fold at the beginning of grain-filling stage grown on Pi-replete soil (Fig. 5C), indicating that the over-expression of *OsPT1* could enhance Pi transportation to shoots even at relative late development stage in rice.

To further characterize the function of OsPT1 in re-translocation of Pi in the aerial part, the change of Pi concentrations was detected in the 1^{st}, 2^{nd} and 3^{rd} leaves ordered from the top at the maturity stage of Pi-replete rice. The results showed that the Pi concentration of the 1^{st} and 2^{nd} leaves of *OsPT1*-Ox plants remained higher than those of WT (Fig. 6), while the P concentrations in the 3^{rd} leaves of *OsPT1*-Ox plants were similar to WT over the period (Fig. 6).

Pi uptake-elicited changes in the root cell membrane potential by over-expression or knockdown of *OsPT1*

To detect the instantaneous Pi transport into root cells in *OsPT1*-Ox, *OsPT1*-Ri and WT plants, we monitored the responses of the cell membrane potential of the roots to $H_2PO_4^-$ treatment. Provision of 300 μM of Pi in the bathing solution elicited a rapid membrane potential depolarization of WT root cells, confirming that anion Pi transport into the cells through nH^+/Pi co-transporters (Ullrich-Eberius et al., 1984; Tamai et al., 1985). The Pi-uptake induced instantaneous depolarization of the root cells in *OsPT1*-Ox on the average was nearly 2-and 4-fold of that of WT and *OsPT1*-Ri, respectively (Fig. 7). These findings are consistent with the data showing that the highest uptake rate was in *OsPT1*-Ox plants, the lowest in *OsPT1*-Ri plants, and middle in WT in Fig. 5A.

Change in the expression of *OsPT1* affected the root growth and root hair development

As commonly observed in other Pi-deficient plant roots, the roots of WT, *OsPT1*-Ox lines and *OsPT1*-Ri lines developed large number of root hairs toward the apical ends, and there were slightly shorter root hairs in the transgenic lines than in WT under Pi-deficient condition (Fig. 8B, C and D). However, the number and length of root hairs developed from *OsPT1*-Ox lines were 5-fold more than that of WT grown at Pi-sufficient solution (Fig. 8). *OsPT1*-Ri lines also increased the root hair occurrences in comparison with WT grown at the Pi- sufficient level (Fig. 8A, C and D).

The expression of *OsPT1* was up-regulated in rice Pi accumulator mutant (*ospho2*) and not altered in Pi starvation **responsive mutant (*osphr2*)**

It has been previously reported that mutation of a Pi accumulator gene (*OsPHO2*) in rice resulted in excess of Pi in its shoots, while Pi concentration in the roots was not largely affected (Wang et al., 2009; Hu et al., 2011). Since the *OsPT1*-Ox phenotype was similar to that of *ospho2* under Pi-sufficient condition, we examined the expression of *OsPT1* in *ospho2* mutant plants using the real time quantitative RT-PCR. Interestingly, *OsPT1* transcripts in the shoots were 2.5- and 6-fold more in *ospho2* mutant than in WT under the Pi-sufficient and -deficient conditions, respectively (Fig. 9A). *OsPT1* expression in the roots was also significantly up-regulated by the mutation of *OsPHO2* irrespective of Pi supply levels (Fig. 9A). In rice, Phosphate Starvation Response 2 (*OsPHR2*) has been characterized as an ortholog gene of *Arabidopsis AtPHR1* and functions in Pi responsive signaling pathway (Zhou et al., 2008). However, we did not observe a significant change of *OsPT1* expression in both *osphr2* roots and shoots in comparison with WT (Fig. 9B).

Discussion

OsPT1 is abundantly expressed in various tissues irrespective of Pi supply condition

Among all Pi transporters belonging to the families of Pht1, Pht2, Pht3 and Pht4 in plants (Rausch and Bucher, 2002), the Pht1 family members were most widely studied due to their vital roles in Pi acquisition from soils and translocation from roots to other parts of plants. Most of Pht1 family members are root-specific Pi transporters, and they were reported to express in root epidermis cells (Mudge et al., 2002; Rae et al., 2003) or in cortical cells after arbuscular mycorrhiza fungi (AMF) colonization (Bucher, 2007). Rice genome contains total 13 members of Pht1 family, two of which (*OsPT11* and *OsPT13*) are AMF colonization enhanced PiTs (Paszkowski et al., 2002; Glassop et al., 2007). We have previously shown that *OsPT2* and *OsPT6* are strongly activated by Pi-starvation with distinct localization and transport function (Ai et al., 2009), while *OsPT8* is a gene that encodes a high affinity PiT and acts as downstream of OsPHR2 with a weak but distinct up-regulation in various tissue organs (Jia et al., 2011). In this work, the analyses of promoter-GUS expression patterns, qRT-PCRs and *in situ* hybridization showed that *OsPT1* was abundantly expressed at various tissues, including roots, root-shoot junctions and leaves irrespective of Pi supply (Fig. 1).

That *OsPT1* expression was not responsive to Pi-deficient condition is consistent with the results of the sequence alignment analysis. Previous studies illustrated that many Pht1 genes from *Arabidopsis*, barley, wheat and rice were activated by AtPHR1 under Pi-deprivation through the conserved P1BS (PHR1 Binding Sequence) element present in their promoters (Rubio et al., 2001; Schunmann et al., 2004; Tittarelli et al., 2007; Ai et al., 2009). We used the motif-building program MEME to identify conserved candidate regulatory motifs shared by the Pi-regulated phosphate transporters among the 13 Pht1 members in rice genome. The predictions indicate that *OsPT1* and *OsPT4*/*OsPT10* in all 13 rice Pht1 gene promoters have no P1BS motifs (Fig. S5). *OsPT2* and *OsPT6*, which were expressed abundantly under Pi starvation in rice contain P1BS motifs in their promoters (Paszkowski et al., 2002; Ai et al., 2009).

It has been confirmed that OsPHR2 is involved in Pi-starvation signaling and regulates the expression of several genes that encode Pi-transporters belonging to Pht1 family in rice (Zhou et al., 2008). That the transcriptional expression of *OsPT1* was not regulated by external Pi-supply level could be further supported by non-altered expression of *OsPT1* in *osphr2* mutant (Fig. 9). This suggests that OsPT1 is not directly regulated by OsPHR2 in rice.

OsPT1 functions in Pi acquisition and distribution, Pi-mediated root hair development in Pi-replete rice

It is generally accepted that Pi uptake of roots from low Pi soil solution is catalysed by high-affinity PiTs (Raghothama, 1999). It has been shown that AtPht1;1 and AtPht1;4, which were most highly expressed in the epidermis and root hair cells, contributed to Pi transport into roots during growth in a wide range of external Pi concentrations (Shin et al., 2004), while AtPht1;5 which showed Pi deficiency-induced expression specifically in the phloem cells of older leaves, cotyledons, and flowers (Mudge et al., 2002) functions in mobilizing Pi between source and sink organs (Nagarajan et al., 2011). The *OsPT1* promoter directed its constitutive expression in epidermis, cortex and stele cells of various rice tissues (Fig. 1) suggests that OsPT1 is likely to be involved both in Pi acquisition and translocation. However, either over-expression or knockdown of *OsPT1* did not significantly affect shoot biomass, Pi concentration in both roots and shoots, and Pi distribution at deficient-Pi supplied rice (Fig. 3, 4). There were only slight differences of the root responses to Pi-starvation in the transgenic rice in comparison to WT (Fig. 8). It has been shown that Pi-starvation in rice strongly enhanced expression of high affinity Pi-transporter gene *OsPT6* which was expressed in multiple cell types from epidermis, cortex to stele, and low affinity Pi-transporter gene *OsPT2* which was exclusively expressed in stele cells of various rice tissues (Ai et al., 2009). Therefore, it could be assumed that OsPT1 has the functional redundancy with other Pi-starvation up-regulated Pht1 members for acquisition and transportation of Pi. Enhanced expression of *OsPT2* and *OsPT6*, possibly together with other non-characterized Pht1 members, could compensate the altered expression of *OsPT1* in the Pi-starved rice plants.

Maintaining sufficient Pi in plant above ground parts depends not only on root Pi acquisition from external solution, but also on transfer of Pi from roots to shoots *via* xylem and re-distribution inside the plant *via* phloem. PHO1 protein primarily expressed in root vascular cylinder is known in mediating Pi efflux for loading Pi to root xylem in *Arabidopsis* (Hamburger et al., 2002; Stefanovic 2011). In rice, it has been shown that OsPHO1;2 plays an important role in transferring Pi from roots to shoots (Secco et al., 2010). However, it is not clear if Pht1 members are directly responsible for Pi loading or unloading or retrieval in the vascular tissue, particularly under Pi-sufficient condition. Gómez-Ariza et al. (2009) analyzed the expression of five tomato Pi transporter genes in the different root tissues using the laser microdissection technology. The results indicated that no expression of the detected Pi transporter genes was observed in the central cylinder, irrespective of the presence of the arbuscular symbiosis. Previously, we showed that knockdown of *OsPT2* exclusively expressed in Pi-starved root stele cells decreased Pi transport from roots to shoots in rice (Ai et al., 2009). In the present work, the increase of Pi-supply gradually enlarged the difference of shoot P concentration between the transgenic rice and WT, and thus resulted in significantly higher P in *OsPT1*-Ox and lower P in *OsPT1*-RNAi mutants (Fig. 4). *OsPT1*-Ox had significantly higher root cell membrane potential depolarization responses to external Pi and higher Pi concentration in xylem sap than WT under P-replete condition (Fig. 5, 7). It is also interesting that over-expression of *OsPT1* resulted in much higher Pi in young leaves of mature plants (Fig. 6). All these data demonstrated that OsPT1 is involved in root Pi uptake and allocation in Pi-replete rice.

In *Arabidopsis*, over-expression of *AtPht1;5* lead to increases of root hair numbers and length both under Pi-sufficient and -deficient conditions, while silencing of the gene did not have significant effect on the root hair development (Nagarajan et al., 2011). It was remarkable that the *OsPT1*-Ri lines, particularly *OsPT1*-Ox lines, developed much longer and dense root hairs only under P-replete condition (Fig. 8). Since there was no significant difference of Pi concentration in their roots under Pi-sufficient condition (Fig. 3C), the enhanced growth of root hair length and number of *OsPT1*-Ox in Pi-sufficient medium (Fig. 8) could not be simply explained by internal Pi status induced changes of root growth. This could be due to differential distribution of P between different tissues and organs in the whole plants by OsPT1 leading to altered root hair development.

OsPT1 and *OsPT8* have similar expression pattern but different regulation pathways

Of the 13 Pi transporter members belonging to Pht1 family in rice, *OsPT1* and *OsPT8* were the most highly expressed in both roots and shoots grown at high Pi level (Jia, et al., 2011; Fig. 1A). The analyses of GUS reporter driven by the promoters of *OsPT1* and *OsPT8* genes indicate a partial overlap in their spatial expression patterns with the strongest expression in the epidermis, cortical and stele cells (Jia, et al., 2011; Fig. 1B). However, unlike *OsPT1*, the promoter of *OsPT8* contains P1BS element and its transcripts could be enhanced by Pi-starvation and by over-expression of *OsPHR2* (Jia et al., 2011). In addition, *OsPT1*, but not *OsPT8*, was strongly up-regulated in *ospho2* mutant, a shoot Pi-over-accumulator (Fig. 9; Jia et al., 2011). Its interaction with OsPHO2 signaling pathway needs to be characterized next.

Over-expression of *OsPT8* resulted in excessive Pi in both roots and shoots leading to Pi toxicity symptoms under high Pi supply condition (Jia et al., 2011), whereas over-expression of *OsPT1* increased Pi accumulation only in the shoots under Pi-sufficient condition (Fig. 3). Interestingly, constitutive enhanced *OsPT1* expression up-regulated *OsPT8* with concurrent down-regulation of other several Pht1 members including *OsPT2* and *OsPT6* in the shoots (Fig. S3), while *OsPT8*-knockdown mutation decreased *OsPT1* expression (Jia, et al., 2011). In contrast, over-expression of *OsPT8* did not affect the expression of *OsPT1*, but enhanced expression of *OsPT2* and *OsPT5* largely in the shoot (Jia et al., 2011). These results imply a possible functional interaction between *OsPT1* and *OsPT8*, which will be elucidated by the double mutant of these two genes in the future.

In conclusion, this work shows that OsPht1;1 (OsPT1) is a key member of Pht1 family involved in Pi uptake and translocation in rice under Pi-replete condition. It was expressed abundantly and constitutively in various cell types of both roots and shoots, irrespective of Pi-supply level. This strengthens our understanding of the PTs function during Pi-sufficient condition in higher plants.

Material and Method

Plant materials and growth conditions

The *Oryza sativa* L. ssp. *japonica* variety Nipponbare was used for the physiological experiments and rice transformation.

For hydroponic experiments, the seed sterilization procedure and the basal nutrient solution composition for seedling growth in a glasshouse were as described previously (Li et al., 2006). The 10d old seedlings were transferred to nutrient solution containing 1.25mM NH_4NO_3, 0.35mM K_2SO_4, 1mM $CaCl_2 \cdot 2H_2O$, 1mM $MgSO_4 \cdot 7H_2O$, 0.5mM $Na_2SiO_3 \cdot 9H_2O$, 20μM Fe-EDTA, 20μM H_3BO_3, 9μM $MnCl_2 \cdot 4H_2O$, 0.32μM $CuSO_4 \cdot 5H_2O$, 0.77μM $ZnSO_4 \cdot 7H_2O$ and 0.39μM $Na_2MoO_4 \cdot 2H_2O$, supplemented with 300 μM Pi (Pi-sufficient) or 10 μM Pi (Pi-deficient). The Hydroponic experiments were carried out in a growth room with 16h light (30℃)/8h dark (22℃) photoperiod and the relative humidity was controlled at ~70%. Initial pH of the solution was adjusted to 5.5, and deionized water was used throughout the experiments. The nutrient solution was replaced every other day.

Samples were collected after the plants were treated for three weeks for semi-quantitative reverse transcription (RT)-PCR and real time quantitative RT-PCR, histochemical localization of the reporter gene and the Pi uptake assay. In the experiments involving transgenic plants, the seeds were geminated and screened in a solution containing 25 mg L^{-1} hygromycin for 7 days before transferred to the hydroponics system. For the different Pi concentration treatments, 300, 200, 80 and 10 μM Pi were used in the culture solution. For each experiment, three to five biological replicates were harvested.

The rice *Tos17* insertion mutants *ospho2* (NE8038_0_102_1A) and rice T-DNA insertion mutants *osphr2* (04Z11NL88) were obtained from the National Institute of Agrobiological Sciences, Functional Genomics Laboratory (Japan), National Key Laboratory of Crop Genetic Improvement, National Center of Plant Gene Research, Huazhong Agricultural University, Wuhan, China (RMD, http://rmd.ncpgr.cn), respectively. The confirmed homozygous mutant seedlings were used for the detection of the expression levels of *OsPT1*. The conditions of growth were the same as described above.

Generation of the transgenic plants

For GUS expression pattern driven by the native promoter of *OsPT1*, the upstream sequence of the coding region of *OsPT1* was first PCR amplified from the genomic DNA of *Oryza sativa* L. ssp. *japonica* variety Nipponbare, using the primers listed in Table S1. The restriction sites were incorporated into the primers to facilitate cloning into the expression vector. The amplified DNA fragments were cloned into the pMD19-T vector (TaKaRa), and were confirmed by restriction enzyme digestion and DNA sequencing. After digesting with the pMD19-T vector, the native promoter fragment of *OsPT1* was cloned with the GUS reporter genes into the binary vectors pS1aG-3 (kindly provided by Dr. Delhaize, CSIRO Plant Industry, http://www.pi.csiro.au). The expression pattern driven by ubiquitin promoter was used as the positive control.

For *OsPT1*-Ox transgenic plants, the cauliflower mosaic virus 35S promoter was used. The expression vector used was pCAMBIA1302. The primers for amplifying the coding region sequence were listed in Table S1. The procedures for *OsPT1*-RNAi transgenic plants were as described previously (Ai et al., 2009). A 255-bp fragment of *OsPT1* coding sequence was amplified using the specific primers listed in Table S1. The expression vector was transferred to *Agrobacterium tumefaciens* strain EHA105 by electroporation, and were transformed into rice as described by Upadhyaya et al. (2000).

Semi-quantitative RT-PCR and quantitative real-time PCR

Total RNAs were prepared from the roots and shoots of wild type or *OsPT1*-Ox or *OsPT1*-Ri using TriZol reagent (Invitrogen, http://www.invitrogen.com). Semi-quantitative RT-PCR for an *actin* (26 cycles) and *OsPT1*(28 cycles) were performed using gene-specific primers. The PCR products were loaded on 1.2% agarose gels and photographed using a CCD camera.

For quantitative PCR analysis, DNase I-treated total RNAs were used for reverse transcription using SuperScript II (Invitrogen). The cDNA samples were diluted to 1, 0.5 and 0.1 ng/mL. Triplicate quantitative assays were performed on each cDNA dilution with the SYBR Green Master Mix with an ABI 7000 sequence detection system, according to the manufacturer's protocol (Applied Biosystems, Foster, City, CA); the gene-specific primers were designed by using PRIMEREXPRESS software (Applied Biosystems). The relative quantification method was used to evaluate quantitative variation between replicates examined. The amplification of *OsRAc1* (*actin*) was used as an internal control to normalize all data. Triplicate quantitative assays were performed on each cDNA samples. All primers used for PCR are given in Table S2.

Histochemical localization of GUS expression

The histochemical analysis of GUS activity was examined as described previously (Ai et al., 2009). Briefly, the samples were submersed in GUS reaction mix, and were incubated at 37℃ overnight. To investigate sub-cellular expression patterns, the stained tissues were rinsed and fixed in FAA for 24h, embedded in paraffin and then sectioned. The sections were transferred onto a slide and visualized under a stereomicroscope. The stained or sectioned tissues were photographed using an OLYMPUS MVX10 steromicroscope, with a color CCD camera.

***In situ* hybridization**

For *in situ* hybridization, digoxigenin-labeled DNA probes of antisense and sense *OsPT1* were synthesized by Invitrogen (USA) with the DNA sequences: AGATGACACAAATGGTTAGCGGCAA (antisense) and GCAGTACTCGTATAGCTCATTCTAT (sense). Root and leaf of ten-day-old plantlets of wild-type grown either in the Pi-sufficient (300 μM Pi, +P) or Pi-deficienct (10 μM Pi, -P) conditions were fixed, dehydrated, embedded in paraffin and the sections were prepared as described in Vernoux et al., (2000). The hybridizations were done by Shanghai Lc Biotech Co. China. DIG-labelled probes were detected by anti-DIG conjugated with alkaline phosphatase (AP) and SIGMAFAST Fast Red TR/naphthol AS-MX Tablets (Sigma-Aldrich). The reaction was stopped by adding 10 mM Tris, 5 mM EDTA, pH 7.5. The background color of hybridization was blue. The light yellow color corresponds to the specific signal with antisense probe.

Functional complementation assay of OsPT1 in yeast

The yeast manipulations were performed as described previously (Ai et al., 2009). For the complementation assay, the coding sequence of *OsPT1* was amplified by PCR, and was subcloned into the yeast expression vector p112A1NE to create *OsPT1*-p112A1NE. The construct was transformed into the yeast Pi uptake-defective mutant MB192 (Bunya et al., 1991). The MB192-*OsPT1* and control cells were grown to the logarithmic phase and then subjected to the YNB (yeast nitrogen base) liquid medium containing different Pi concentrations (20, 60, 100 μM) evenly. Bromocresol purple was used as pH indicator. From purple to yellow, the color transformation of the liquid medium represented the acidification.

To detect the pH susceptibility of Pi uptake, different extracellular pHs (4, 5, 6, 6.5, 7, 7.5, 8) were used at a fixed concentration of 80 μM K_2HPO_4. MES was used to keep the stability among the different pH, and measured the value of OD600 after 24h for the yeast strains Yp112- *OsPT1*, wild-type and MB192. For each experiment, five biological replicates were measured.

In order to determine the kinetic properties of the OsPT1 transporter, Pi-uptake experiments using ^{33}Pi were performed using the transformed yeast. About 1 mg fresh yeast cells samples were used following the previous described method (Ai *et al.*, 2009).

Measurement of P concentration in plants

Samples for the transgenic and WT plants from either Pi-sufficient or Pi-deficient treatments were sampled separately. For the measurement of un-assimilated Pi concentration in the plant, about 0.5 g fresh samples were used following the previous described method (Zhou et al., 2008). Briefly, the sample was homogenized in 1 mL 10% (w/v) of perchloric acid using an ice-cold mortar and pestle. The homogenate was then diluted 10 times with 5% (w/v) perchloric acid and placed on ice for 30 min. after centrifugation at 10,000g for 10 min at 4℃, the supernatant was used for Pi measurement *via* the molybdenum blue method. The absorption values for the solution at 650 nm were determined using a Spectroquant NOVA60 spectrophotometer.

For the measurement of total P concentration in the plant, the samples were used following the method described by Wang et al. (2009) and Chen et al. (2007). Briefly, 0.03 g dry samples were pre-digested in glass tubes with H_2SO4 for 2 h. The tubes were then heated to 180℃ and 50μl H_2O_2 was added every 10 min until the solution turned colorless. Pi concentration was analyzed as described above after dilution.

Xylem sap collection was performed at the initial grain-filling stage using the procedures as described previously (Fan et al., 2005). Briefly, the stems were cut at

3-5 cm above the roots. The cut surfaces were rinsed with deionized water and blotted dry. Xylem sap from this cut surface were collected by absorption into a cotton wool pad placed on the cut surface. After 12h, the sap sample in the cotton wool was extracted, and then the water extractable P concentration was measured using the procedures as described above.

Radioactive ^{33}P-uptake experiments

Seedlings of *OsPT1*-Ox, *OsPT1*-Ri and WT plants that had been subjected to Pi -sufficient condition for 3-week were incubated for 12h and 24h in 250 ml of nutrient solutions containing 8μCi of $KH_2{}^{33}PO_4$ (Ai et al., 2009). Plants were rinsed in sterile distilled water until the radioactivity could not be detected in the solution, were blot-dried on 3M filter paper, and the roots and shoots were dried and weighed separately. The tissues were dried at 70°C for 2 days, then wet-digested in a mixture of H_2SO_4 and H_2O_2. The radioactivity of these solutions was measured by a Beckman LS6500 scintillation counter. Autoradiographs of the radioactive seedlings were then developed using photographic film plates.

Plasma membrane potential measurements

Plasma membrane potentials of rice roots were measured as previously described (Fan et al., 2005) with minor modification. A single primary root (not seminal) of intact rice plants was held in a Plexiglas chamber (volume 2.0 mL) and bathed with a flowing solution (containing 5 mM MES, 0.5 mM $CaCl_2$, 0.05 mM KCl, 4mM NaCl and pH 6.0) at the rate of 1 mL per min. The 4 mM NaH_2PO_4 was taken place of 4 mM NaCl as $H_2PO_4^-$ treatment on root during membrane potential recording.

Measurement of Roots and Root Hairs

The number and length of root hairs were measured after 7 d under Pi-sufficient or Pi-deficient conditions. The number of lateral roots and all emerged lateral roots on primary root was counted by naked eye and divided by the respective length of the primary roots. For root hair measurement, the root hair zone immediately behind the root tips was observed under a microscope (Olympus MVX10). The number of root hairs from one side of the root hair zone of primary root was counted. The roots were photographed using an OLYMPUS MVX10 stereomicroscope, with a color CCD camera (Olympuhttp://www.olympus-global.com). Values are averages (±SE) of 10 seedlings.

Accession Numbers

Sequence data from this article can be found in the rice Genome Initiative/GenBank data libraries under accession number AF536961 (*OsPT1*).

Supplementary Data

Supplementary Table S1. Primers used to generate the expression vectors. Restriction site sequences are underlined.

Supplementary Table S2. Primers used to amplify the *OsPT1* cDNA fragments.

Supplementary Figure S1 The transcriptional patterns of *OsPT1* in roots and leaves of rice (*Oryza sativa* L.ssp. *Japonica* cv. Nipponbare).

Supplementary Figure S2 The expression of *OsPT1* driven by the native promoter in reproductive organs of rice.

Supplementary Figure S3 Relative expression of the genes that encode Pi-transporters belonging to Pht1 family in shoot of *OsPT1*-Ox transgenic and wild-type plants.

Supplementary Figure S4 ^{33}Pi uptake in *OsPT1*-Ox, *OsPT1*-Ri and wild type plants.

Supplementary Figure S5 Motif analysis in the putative promoters of genes that encode Pi-transporters belonging to Pht1 family in rice.

LITERATURE CITED

Ai PH, Sun SB, Zhao JN, Fan XR, Xin WJ, Guo Q, Yu L, Shen QR, Wu P, Miller AJ, Xu GH (2009) Two rice phosphate transporters, OsPht1;2 and OsPht1;6, have different functions and kinetic properties in uptake and translocation. Plant J **57:** 798–809

Bucher M (2007) Functional biology of plant phosphate uptake at root and mycorrhiza interfaces. New Phytol **173:** 11–26

Bunya M, Nishimura M, Harashima S, Oshima Y (1991) The *PHO84* gene of *Saccharomyces-cerevisiae* encodes an inorganic-phosphate transporter. Mol Cell Biol **11:** 3229–3238

Chen AQ, Hu J, Sun SB, Xu GH (2007) Conservation and divergence of both phosphate- and mycorrhiza-regulated physiological responses and expression patterns of phosphate transporters in solanaceous species. New Phytol **173:** 817–831

Fan XR, Shen QR, Ma ZQ, Zhu HL, Yin XM, Miller AJ (2005) A comparison of nitrate transport in four different rice (*Oryza sativa* L.) cultivars. Sci China Ser C, **48:** 897–911

Glassop D, Godwin RM, Smith SE, Smith FW (2007) Rice phosphate transporters associated with phosphate uptake in rice colonized with arbuscular mycorrhizal fungi. Can J Bon **85:** 644–651

Gómez-Ariza J, Balestrini R, Novero M, Bonfante P (2009) Cell-specific gene expression of phosphate transporters in mycorrhizal tomato roots. Biol Fertil Soils **45:** 845–853

Hamburger D, Rezzonico E, MacDonald-Comber Petétot J, Somerville C, Poirier Y. (2002) Identification and characterization of the Arabidopsis PHO1 gene involved in phosphate loading to the xylem. Plant Cell **14:**889-902.

Hu B, Zhu CG, Li F, Tang JY, Wang YQ, Lin AH, Liu LC, Che RH, Chu CC (2011) *LEAF TIP NECROSIS 1* plays a pivotal role in the regulation of multiple phosphate starvation responses in rice. Plant Physiol **156:** 1101–1115

Javot H, Penmetsa RV, Terzaghi N, Cook DR, Harrison MJ (2007) A *Medicago truncatula* phosphate transporter indispensable for the arbuscular mycorrhizal symbiosis. Proc Natl Acad Sci USA **104:** 1720–1725

Jefferson RA, Kavanagh TA, Bevan MW (1987) GUS fusions; beta-glucuronidase as a sensitive and versatile gene fusion marker in higher plants. EMBO J **6:** 3901–3907

Jia HF, Ren HY, Gu M, Zhao JN, Sun SB, Zhang X, Chen JY, Wu P, Xu GH (2011) Phosphate transporter gene, *OsPht1;8*, is involved in phosphate homeostasis in rice. Plant Physiol **156:** 1164-1175

Li BZ, Xin WJ, Sun SB, Shen QR, Xu GH (2006) Physiological and molecular responses of nitrogen-starved rice plants to re-supply of different nitrogen sources. Plant Soil **287:** 145–159

Liu F, Wang ZY, Ren HY, Shen C, Li Y, Ling H, Wu CY, Lian XM, Wu P (2010) OsSPX1 suppresses the function of OsPHR2 in the regulation of expression of *OsPT2* and phosphate homeostasis in shoots of rice. Plant J **62:** 508-517

Misson J, Thibaud MC, Bechtold N, Raghothama K, Nussaume L (2004) Transcriptional regulation and functional properties of *Arabidopsis* Pht1;4, a high affinity transporter contributing greatly to phosphate uptake in phosphate deprived plants. Plant Mol Biol **55:** 727–741

Mudge SR, Rae AL, Diatloff E, Smith FW (2002) Expression analysis suggests novel roles for members of the Pht1 family of phosphate transporters in *Arabidopsis*. Plant J **31:** 341–353

Nagarajan VK, Jain A, Poling MD, Lewis AJ, Raghothama KG, Smith AP (2011) *Arabidopsis* Pht1;5 mobilizes phosphate from source to sink organs and influences the interaction between phosphate homeostasis and ethylene signaling. Plant Physiol **156:** 1149–1163

Paszkowski U, Kroken S, Roux C, Briggs SP (2002) Rice phosphate transporters include an evolutionarily divergent gene specifically activated in arbuscular mycorrhizal symbiosis. Proc Natl Acad Sci USA **99:** 13324–13329

Paszkowski U (2006) A journey through signaling in arbuscular mycorrhizal symbioses. New Phytol **172**: 35–46

Plaxton WC, Carswell MC (1999) Metabolic aspects of the phosphate starvation response in plants. In: Lerner HR (ed) Plant responses to environmental stresses: from phytohormones to genome reorganization. Marcel-Dekker, New York, NY, USA, pp 349–372

Preuss CP, Huang CY, Gilliham M, Tyerman SD (2010) Channel-Like characteristics of the low-affinity barley phosphate transporter PHT1; 6 when expressed in *Xenopus Oocytes*. Plant Physiol **152:** 1431–1441

Rae AL, Cybinski DH, Jarmey JM, Smith FW (2003) Characterization of two phosphate transporters from barley; evidence for diverse function and kinetic properties among members of the Pht1 family. Plant Mol Biol **53:** 27–36

Raghothama KG (1999) Phosphate acquisition. Annu Rev Plant Physiol Mol Biol **50:** 665–693

Rausch C, Bucher M (2002) Molecular mechanisms of phosphate transport in plants. Planta **216:** 23–37

Rubio V, Linhares F, Solano R, Martin AC, Iglesias J, Leyva A, Paz-Ares J (2001) A conserved MYB transcription factor involved in phosphate starvation signaling both in vascular plant and in unicellular algae. Gene Dev **15:** 2122– 2133

Schunmann PHD, Richardson AE, Smith FW, Delhaize E (2004) Characterization of promoter expression patterns derived from the Pht1 phosphate transporter genes of barley (*Hordeum vulgare* L.). J Exp Bot **55:** 855–865

Secco D, Baumann A, Poirier Y (2010) Characterization of the rice PHO1 gene family reveals a key role for OsPHO1;2 in phosphate homeostasis and the evolution of a distinct clade in dicotyledons. Plant Physiol **152:** 1693-1704.

Shin H, Shin HS, Dewbre GR, Harrison MJ (2004) Phosphate transport in *Arabidopsis*: Pht1;1 and Pht1;4 play a major role in phosphate acquisition from both low- and high-phosphate environments. Plant J **39:** 629–642

Smith FW, Mudge SR, Rae AL, Glassop D (2003) Phosphate transport in plants. Plant Soil **248**: 71–83

Stefanovic A, Arpat AB, Bligny R, Gout E, Vidoudez C, Bensimon M, Poirier Y (2011) Over-expression of PHO1 in Arabidopsis leaves reveals its role in mediating phosphate efflux. Plant J **66**: 689-99.

Tamai Y, Tohe A, Oshima Y (1985) Regulation of inorganic phosphate transport-systems in *Saccharomyces cerevisiae*. J Bacteriol **164:** 964–968

Tittarelli A, Milla L, Vargas F, Morales A, Neupert C, Meisel LA, Salvo G, Penaloza E, Munoz G, Corcuera LJ, Silva H (2007) Isolation and comparative analysis of the wheat TaPT2 promoter: identification in silico of new putative regulatory motifs conserved between monocots and dicots. J Exp Bot **58:**

2573–2582

Ullrich-Eberius CI, Novacky A, Bel AJE (1984) Phosphate-uptake in *Lemna-gibba* G1-energetics and kinetics**.** Planta **161:** 46–52

Upadhyaya NM, Surin B, Ramm K, Gaudron J, Schunmann PHD, Taylor W, Waterhouse PM, Wang MB (2000) *Agrobacterium*-mediated transformation of Australian rice cultivars Jarrah and Amaroo using modified promoters and selectable markers. Aust J Plant Physiol **27:** 201–210

Vernoux T, Kronenberger J, Grandjean O, Laufs P, Traas J (2000) PIN-FORMED 1 regulates cell fate at the periphery of the shoot apical meristem. Development **127:** 5157–5165

Wang C, Ying S, Huang HJ, Li K, Wu P, Shou HX (2009) Involvement of *OsSPX1* in phosphate homeostatis in rice. Plant J **57**: 895–904

Zhou J, Jiao FC, Wu ZC, Li YY, Wang XM, He X, Zhong WQ, Wu P (2008) OsPHR2 is involved in phosphate–starvation signaling and excessive phosphate accumulation in shoots of plants. Plant Physiol **146:** 1673–1686

Figure legends

Figure 1 Expression pattern and tissue localization of *OsPT1* in Pi-sufficient and -deficient rice.

A, Transcriptional patterns of *OsPT1* in the roots and shoots of rice (*Oryza sativa* L.ssp. *Japonica* cv. Nipponbare).

10-d-old rice seedlings were transferred to the Pi-sufficient (300 µM Pi, +P) and Pi-deficient (10 µM Pi, -P) conditions for 21d. Total RNAs were extracted from roots and shoots of the seedlings and determined by real time quantitative RT-PCR. A housekeeping gene, *actin* (*OsRac1*, accession number AB047313), was used as the internal standard. Error bars indicate SE ($n = 3$) of three biological replicates.

B, The expression pattern of GUS driven by the native promoter of *OsPT1* in rice.

OsPT1 promoter-driven expression of the GUS reporter gene in primary roots (a,b), root-shoot junctions (c,d), leaf blade (e,f); transverse section of the primary roots (g,h,i,j) and leaves (k,l) of the rice seedlings supplied with the Pi-sufficient (300 µM Pi, +P) and Pi-deficient (10 µM Pi, -P) condition for 21d. Transverse sections of the primary roots were at 0.5 cm from the root tips. Ph, X, Ep, Co, En, LRP and Me represents phloem, xylem, epidermis, cortex, endodermis, lateral root primordium and mesophyll cells, respectively.

C, Localization of *OsPT1* expression in the roots and leaves of rice by *in situ* hybridization.

10-d-old rice seedlings were transferred to the Pi-sufficient (300 µM Pi, +P) and Pi-deficient (10 µM Pi, -P) conditions for 21d before tissue collection. Transverse sections of the primary roots were at 0.5 cm from the root tips. Similar signal with Pi-sufficient-Pi or -deficient conditions given by the antisense probe was observed in root (top panel) and leaf (bottom panel) sections. Sense probe was used as the negative control.

Figure 2 Functional expression of *OsPT1* in yeast. A, Complementation of Pi uptake-deficient yeast. Staining test for color reaction in the yeast strains MB192 (control), Yp112-*OsPT1* which contains *OsPT1* in MB192, and wild-type (WT). B, The effects of different pH in the culture medium on the growth of the three yeast strains: Yp112- *OsPT1*, MB192 and WT. Error bars indicate SE (n = 5). C, Velocity of ^{33}Pi transport by transformants containing Yp112-*OsPT1* (closed circles) or carrying a vector (closed square). The non-linear regression of Pi uptake of strain Yp112-*OsPT1* versus external concentration at pH 6.5 was used to estimate the apparent Km value for Pi uptake**.**

Figure 3 The molecular characterization and measurement of P concentration in the transgenic plants under Pi- sufficient and -deficient conditions.

Detection of the expression levels of *OsPT1* in WT and transgenic lines by quantitative RT-PCR (A). Ox1, Ox2, Ri1 and Ri2 represent independent *OsPT1*–Ox and *OsPT1*–Ri lines, respectively. Total RNA was extracted from the roots and leaves in *OsPT1*-Ox, *OsPT1*-Ri and WT plants grown for 21d in the presence of 300 µM Pi (+P) and 10 µM Pi (-P). A housekeeping gene, *actin*, was used as the internal standard. The results are the mean**±**SE of five biological replicates. P concentration of the shoots (B) and roots (C) of the WT and transgenic lines under Pi- sufficient and -deficient conditions were measured. Error bars indicate SE (n = 5).

Figure 4 Pi concentrations of *OsPT1*-Ox and *OsPT1*-Ri lines under different Pi levels in solution culture.

OsPT1-Ox, *OsPT1*-Ri and WT plants were grown for 21d under varying concentrations of Pi (300, 200, 80, 10 µM Pi) in the hydroponic culture, respectively. Pi concentrations of the shoots (A) and roots (B) of *OsPT1*-Ox, *OsPT1*-Ri and wild type plants were measured. Error bars indicate SE (n = 5).

Figure 5 The rate of Pi uptake by roots and the transportation of root acquired Pi to shoots using ^{33}Pi isotope, and the Pi concentration in the xylem sap of rice plants.

OsPT1-Ox, *OsPT1*-Ri and wild-type plants were grown for 7d and then transferred into Pi-sufficient (300 µM Pi) medium. The Pi uptake of these seedlings was monitored over 24h. A, Pi uptake rate of the roots in WT and the transgenic plants on the root dry weight (DW) basis. B, the ratio of accumulated ^{33}P in the shoots to that in the roots of WT and the transgenic plants. C, Pi concentration in the xylem sap of *OsPT1*-Ox and wild-type plants at the grain-filling stage grown in high available Pi soil. Five plants per line were measured. Error bars represent SE (n = 5).

Figure 6 Total P concentration in the different leaves of rice at maturity stage.

Both *OsPT1*-Ox and WT plants were pot-grown under Pi-sufficient condition. The 1^{st}, 2^{nd} and 3^{rd} leaves were ordered from the top at the maturity stage. Error bars indicate SE (n = 5).

Figure 7 Membrane potential changes (ΔE_m) in root rhizodermal cells of *OsPT1*-Ox, *OsPT1*-Ri and WT plants.

Rice seedlings were grown in the solution containing 300 µM Pi for two weeks before the electrophysiological measurements. A, wild type (left), *OsPT1*-Ox plants (middle) and *OsPT1*-Ri plants (right) treated with phosphate, In: 4mM $H_2PO_4^-$ treatment to root; Out: removing 4 mM $H_2PO_4^-$ with 4 mM Cl^-. B, The average values of membrane potential shifts by 4 mM $H_2PO_4^-$ treatments in 12 individual seedlings of WT, *OsPT1*-Ox and *OsPT1*-Ri. Error bars indicate SE (n = 3).

Figure 8 Root phenotypes of WT *OsPT1*-Ox and *OsPT1*-Ri seedlings under Pi-sufficient (+P) and Pi-deficient (-P) conditions.

A and B shows root hair proliferation of WT, *OsPT1*-Ri1 and *OsPT1*-Ox1 of 7-day-old seedlings grown under the presence of 300 µM Pi (A) and 10 µM Pi (B) conditions. The scale bars in the panels represent 0.5 mm. C and D shows the root hair number and length, respectively, which were taken under Pi-sufficient and -deficient conditions. Error bars indicate SE (n = 10).

Figure 9 The expression levels of *OsPT1* in the roots and shoots of *ospho2* and *osphr2* mutants.

10-d-old *ospho2* (A) and WT seedlings were transferred to the Pi-sufficient (300 µM, + Pi) and Pi-deficient (10 µM Pi, -P) conditions for 21d. 10-d-old *osphr2* (B) and WT seedlings were subjected to Pi-sufficient (300 µM Pi, +P) solution. RNA was extracted from roots and leaves of rice plants and the expression levels of *OsPT1* were determined by the quantitative real-time PCR. A housekeeping gene, *actin* (*OsRac1*, accession number AB047313), was used as the internal standard. Error bars indicate SE (n = 3) of three biological replicates.

Figure 1

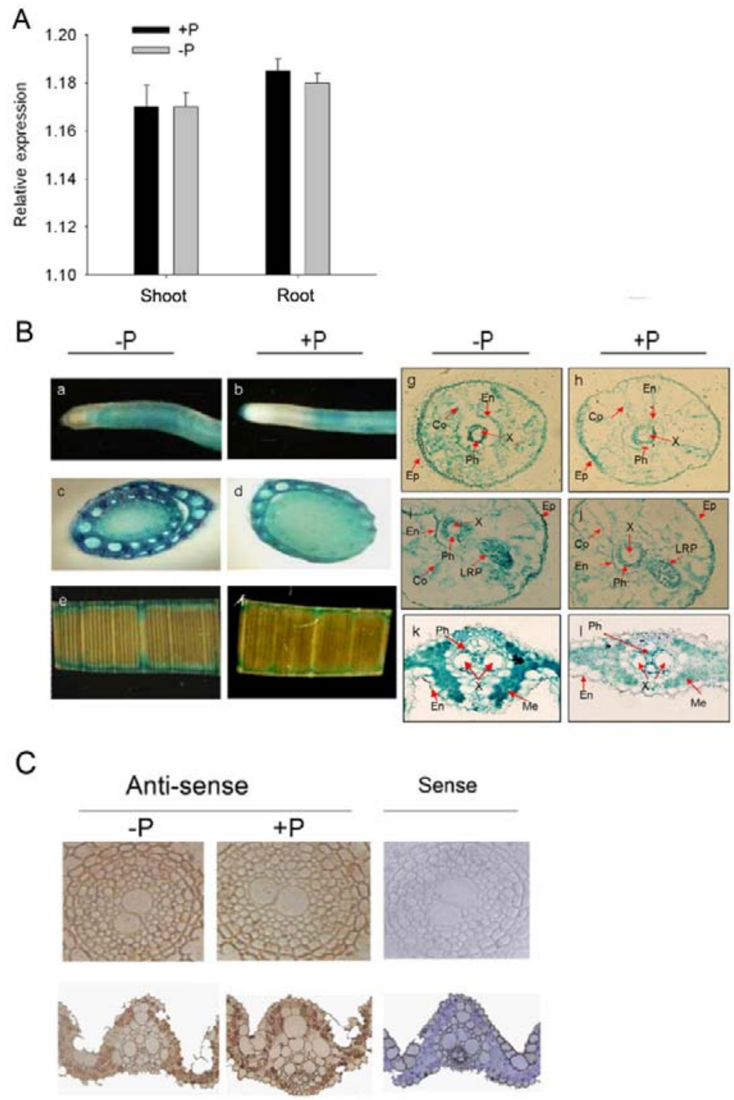

Figure 1 Expression pattern and tissue localization of *OsPT1* in Pi-sufficient and -deficient rice.

A, Transcriptional patterns of *OsPT1* in the roots and shoots of rice (*Oryza sativa* L.ssp. *Japonica* cv. Nipponbare).

10-d-old rice seedlings were transferred to the Pi-sufficient (300 µM Pi, +P) and Pi-deficient (10 µM Pi, -P) conditions for 21d. Total RNAs were extracted from roots and shoots of the seedlings and determined by real time quantitative RT-PCR. A housekeeping gene, *actin* (*OsRac1*, accession number AB047313), was used as the internal standard. Error bars indicate SE (*n* = 3) of three biological replicates.

B, The expression pattern of GUS driven by the native promoter of *OsPT1* in rice.

OsPT1 promoter-driven expression of the GUS reporter gene in primary roots (a,b), root-shoot junctions (c,d), leaf blade (e,f); transverse section of the primary roots (g,h,i,j) and leaves (k,l) of the rice seedlings supplied with the Pi-sufficient (300 µM Pi, +P) and Pi-deficient (10 µM Pi, -P) condition for 21d. Transverse sections of the primary roots were at 0.5 cm from the root tips. Ph, X, Ep, Co, En, LRP and Me represents phloem, xylem, epidermis, cortex, endodermis, lateral root primordium and mesophyll cells, respectively.

C, Localization of *OsPT1* expression in the roots and leaves of rice by *in situ* hybridization.

10-d-old rice seedlings were transferred to the Pi-sufficient (300 µM Pi, +P) and Pi-deficient (10 µM Pi, -P) conditions for 21d before tissue collection. Transverse sections of the primary roots were at 0.5 cm from the root tips. Similar signal with Pi-sufficient-Pi or -deficient conditions given by the antisense probe was observed in root (top panel) and leaf (bottom panel) sections. Sense probe was used as the negative control.

Figure 2

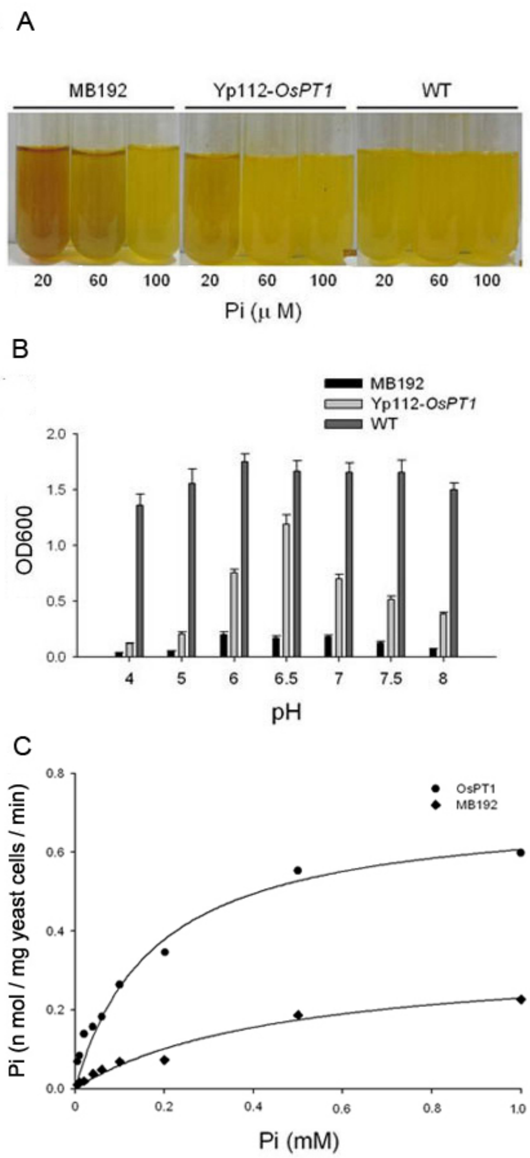

Figure 2 Functional expression of *OsPT1* in yeast. A, Complementation of Pi uptake-deficient yeast. Staining test for color reaction in the yeast strains MB192 (control), Yp112-*OsPT1* which contains *OsPT1* in MB192, and wild-type (WT). B, The effects of different pH in the culture medium on the growth of the three yeast strains: Yp112- *OsPT1*, MB192 and WT. Error bars indicate SE (n = 5). C, Error bars indicate SE (n = 5). C, Velocity of ^{33}Pi transport by transformants containing Yp112-*OsPT1* (closed circles) or carrying a vector (closed square). The non-linear regression of Pi uptake of strain Yp112-*OsPT1* versus external concentration at pH 6.5 was used to estimate the apparent *K*m value for Pi uptake**.**

Figure 3

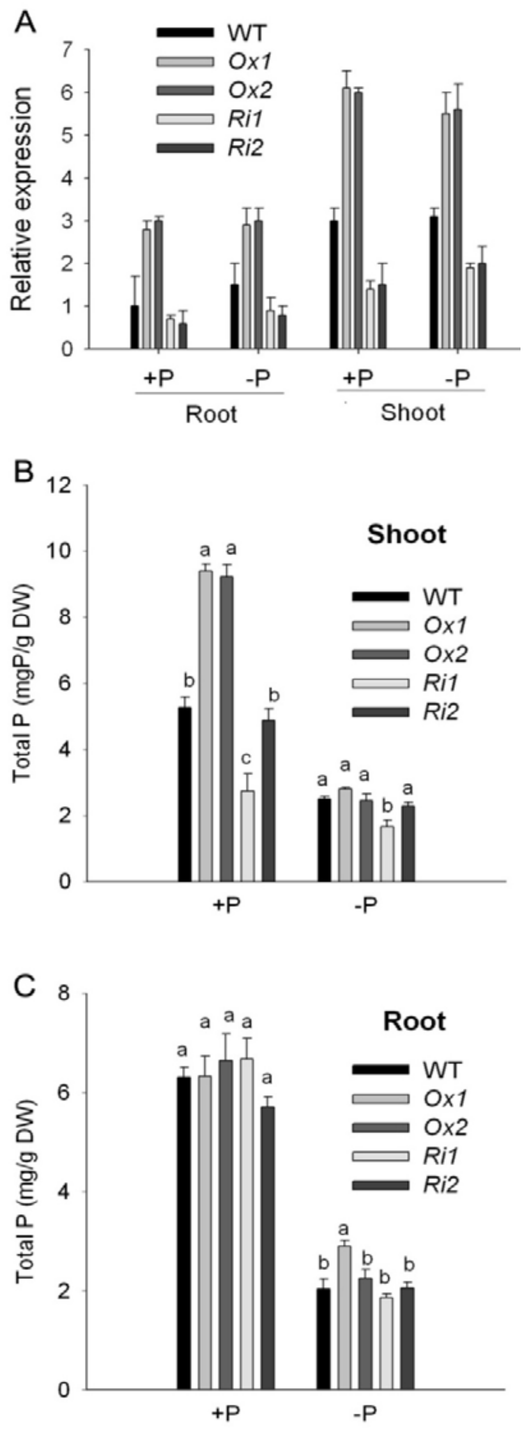

Figure 3 The molecular characterization and measurement of P concentration in the transgenic plants under Pi- sufficient and -deficient conditions.

Detection of the expression levels of *OsPT1* in WT and transgenic lines by quantitative RT-PCR (A). Ox1, Ox2, Ri1 and Ri2 represent independent *OsPT1*–Ox and *OsPT1*–Ri lines, respectively. Total RNA was extracted from the roots and leaves in *OsPT1*-Ox, *OsPT1*-Ri and WT plants grown for 21d in the presence of 300 μM Pi (+P) and 10 μM Pi (-P). A housekeeping gene, *actin*, was used as the internal standard. The results are the mean±SE of five biological replicates. P concentration of the shoots (B) and roots (C) of the WT and transgenic lines under Pi- sufficient and -deficient conditions were measured. Error bars indicate SE (n = 5).

Figure 4

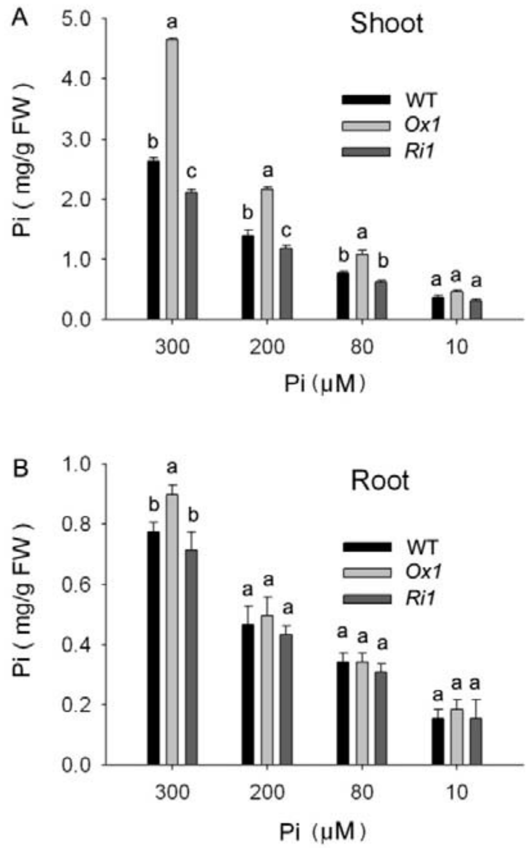

Figure 4 Pi concentrations of *OsPT1*-Ox and *OsPT1*-Ri lines under different Pi levels in solution culture.

OsPT1-Ox, *OsPT1*-Ri and WT plants were grown for 21d under varying concentrations of Pi (300, 200, 80, 10 µM Pi) in the hydroponic culture, respectively. Pi concentrations of the shoots (A) and roots (B) of *OsPT1*-Ox, *OsPT1*-Ri and wild type plants were measured. Error bars indicate SE (n = 5).

Figure 5

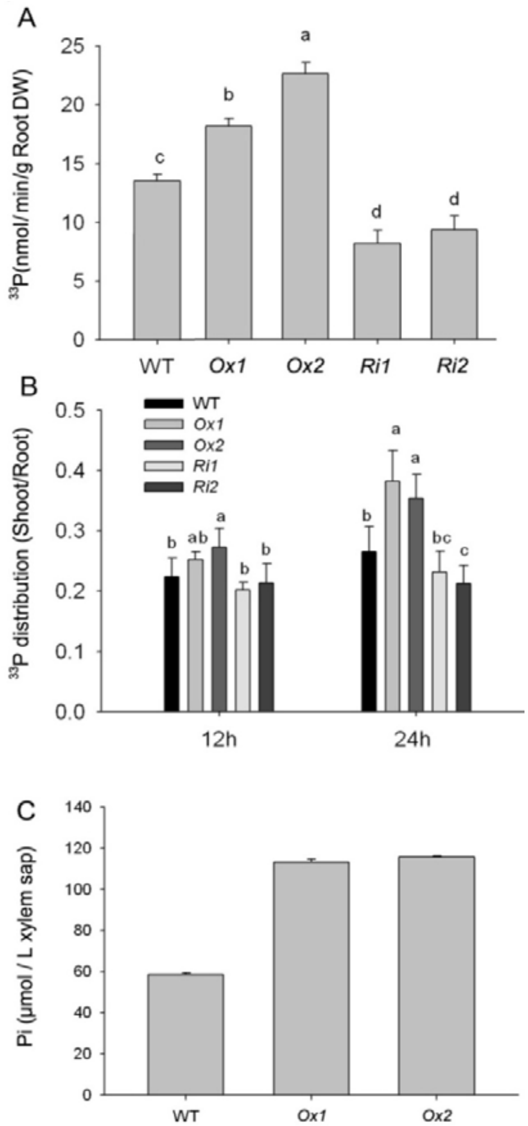

Figure 5 The rate of Pi uptake by roots and the transportation of root acquired Pi to shoots using ^{33}Pi isotope, and the Pi concentration in the xylem sap of rice plants.

OsPT1-Ox, *OsPT1*-Ri and wild-type plants were grown for 7d and then transferred into Pi-sufficient (300 µM Pi) medium. The Pi uptake of these seedlings was monitored over 24h. A, Pi uptake rate of the roots in WT and the transgenic plants on the root dry weight (DW) basis. B, the ratio of accumulated ^{33}P in the shoots to that in the roots of WT and the transgenic plants. C, Pi concentration in the xylem sap of *OsPT1*-Ox and wild-type plants at the grain-filling stage grown in high available Pi soil. Five plants per line were measured. Error bars represent SE (n = 5).

Figure 6

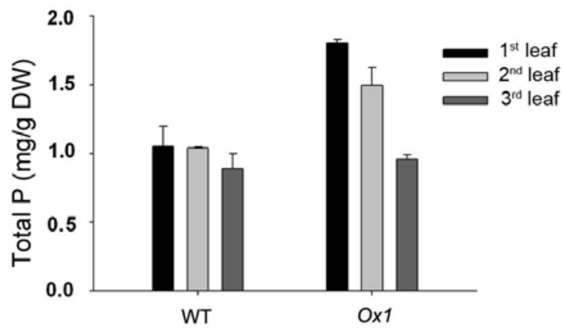

Figure 6 Total P concentration in the different leaves of rice at maturity stage.

Both *OsPT1*-Ox and WT plants were pot-grown under Pi-sufficient condition. The 1st, 2nd and 3rd leaves were ordered from the top at the maturity stage. Error bars indicate SD (n = 5).

Figure 7

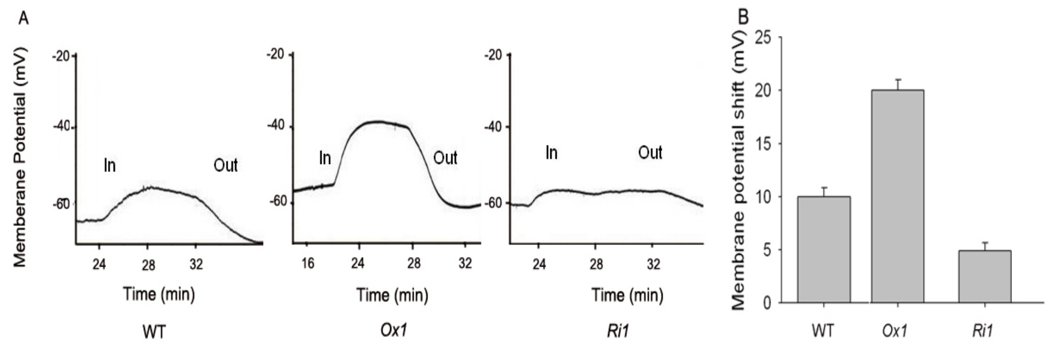

Figure 7 Membrane potential changes (ΔE_m) in root rhizodermal cells of *OsPT1*-Ox, *OsPT1*-Ri and WT plants.

Rice seedlings were grown in the solution containing 300 µM Pi for two weeks before the electrophysiological measurements. A, wild type (left), *OsPT1*-Ox plants (middle) and *OsPT1*-Ri plants (right) treated with phosphate, In: 4mM $H_2PO_4^-$ treatment to root; Out: removing 4 mM $H_2PO_4^-$ with 4 mM Cl^-. B, The average values of membrane potential shifts by 4 mM $H_2PO_4^-$ treatments in 12 individual seedlings of WT, *OsPT1*-Ox and *OsPT1*-Ri. Error bars indicate SE (n = 3).

Figure 8

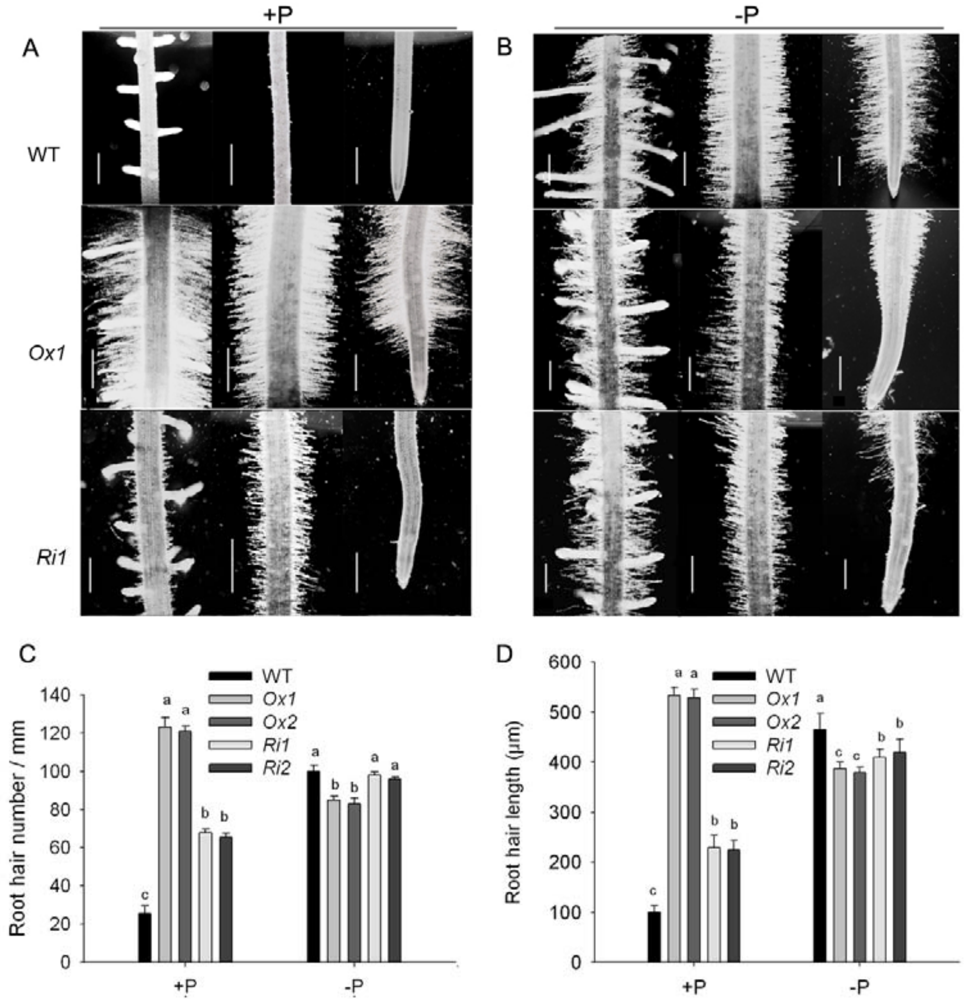

Figure 8 Root phenotypes of WT *OsPT1*-Ox and *OsPT1*-Ri seedlings under Pi-sufficient (+P) and Pi-deficient (-P) conditions.

A and B shows root hair proliferation of WT, *OsPT1*-Ri1 and *OsPT1*-Ox1 of 7-day-old seedlings grown under the presence of 300 µM Pi (A) and 10 µM Pi (B) conditions. The scale bars in the panels represent 0.5 mm. C and D shows the root hair number and length, respectively, which were taken under Pi-sufficient and -deficient conditions. Error bars indicate SE (n = 10).

Figure 9

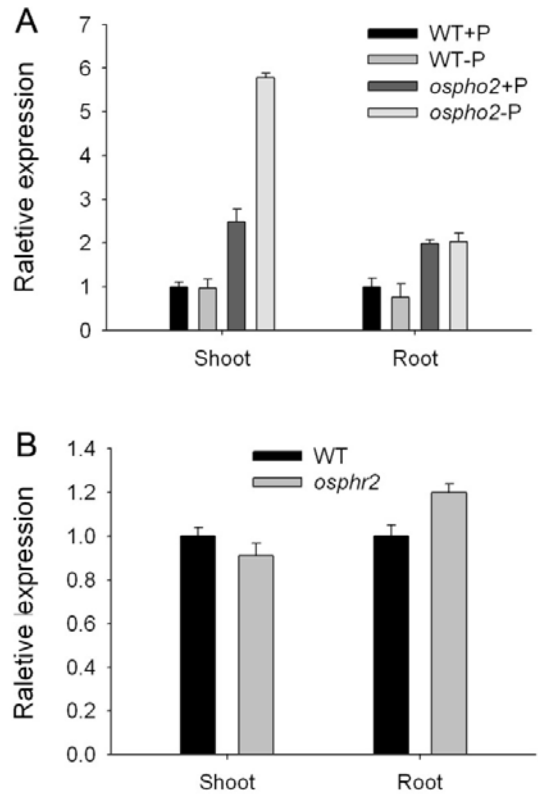

Figure 9 The expression levels of *OsPT1* in the roots and shoots of *ospho2* and *osphr2* mutants.

10-d-old *ospho2* (A) and WT seedlings were transferred to the Pi-sufficient (300 µM, + Pi) and Pi-deficient (10 µM Pi, -P) conditions for 21d. 10-d-old *osphr2* (B) and WT seedlings were subjected to Pi-sufficient (300 µM Pi, +P) solution. RNA was extracted from roots and leaves of rice plants and the expression levels of *OsPT1* were determined by the quantitative real-time PCR. A housekeeping gene, *actin* (*OsRac1*, accession number AB047313), was used as the internal standard. Error bars indicate SE (n = 3) of three biological replicates.